

Excitation and decay of aluminum bulk plasmons at the aluminum/copper phthalocyanine interfaceGianluca Di Filippo,^{1,*} Marco Sbroscia,¹ Giovanni Stefani,¹ Robert A. Bartynski,² and Alessandro Ruocco¹¹*Dipartimento di Scienze, Università degli Studi Roma Tre, via della Vasca Navale 84, I-00146 Rome, Italy*²*Department of Physics and Astronomy and Laboratory for Surface Modification, Rutgers University, Frelinghuysen Road 136, Piscataway, New Jersey 08854, USA*

(Received 7 May 2018; published 12 June 2018)

We present the results of an experiment aimed at studying the archetypal properties of the aluminum bulk plasmon at an organic/metal interface. Electron-electron coincidence spectroscopy is used to determine the contribution of aluminum bulk plasmon decay to the ionization of a thin copper phthalocyanine film. The latter directly depends on the amplitude of the bulk plasmon electric field (generated in the metal substrate) protruding inside the molecular overlayer. The emission of low-energy electrons from the clean substrate is dominated by plasmon-assisted ionization events. These events are not observed when the molecules are adsorbed onto the surface. Our findings suggest that, for the considered system, the bulk plasmon wave is confined within the medium in which it is generated and the interaction of the plasmon field with electrons located in the molecular overlayer does not lead to the emission of low-energy electrons.

DOI: [10.1103/PhysRevB.97.235420](https://doi.org/10.1103/PhysRevB.97.235420)**I. INTRODUCTION**

The quantum of elementary excitation associated with the coherent oscillation of the valence-band electrons of a solid is called a plasmon. The term was first introduced in 1956 by Pines due to the resemblance of these collective modes to the electronic plasma oscillations in gaseous discharges [1]. Plasmons are commonly distinguished as either bulk or surface modes. A bulk plasmon (BP) is a longitudinal wave that propagates through the volume of the metal. The wave produces electron density variations along its direction of propagation. A surface plasmon (SP) corresponds to an electromagnetic wave propagating along a solid/vacuum interface [2]. The induced charge density is such that the component of the plasmon electric field perpendicular to the interface is enhanced near the surface and exponentially decays with distance with a penetration depth of the order of the plasmon wavelength on the vacuum side and one order of magnitude lower on the metal side due to the skin effect [3]. This strong, confined electric field is responsible for several plasmon-mediated enhancement phenomena with applications in the fields of optoelectronics [4,5], energy storage and conversion [6–8], and biosensing [9]. Detailed knowledge of plasmon excitation and decay mechanisms is therefore of crucial relevance in order to improve efficiency of many phenomena that constitute background to technologically important processes, such as energetically demanding chemical reactions [10], photovoltaic devices [11], and photoelectrochemical systems [12].

Despite the vast amount of literature on the investigation of surface plasmons, less attention has been devoted to the study of bulk plasmons. In particular not too much is known about the characteristics of bulk oscillations at the boundary between a metal and a dielectric medium. One question which

is not answered yet is whether the bulk plasmon wave is confined within the medium in which it is generated or whether its influence can extend beyond the surface. In this paper we address this question by investigating the spectrum of low-energy electrons (LEEs) generated by a bulk plasmon decay when a thin molecular film is deposited onto the metal surface.

It is well established that both bulk and surface plasmons can undergo a nonradiative decay through the transfer of a plasmon quantum to a single electron-hole pair. The decay acts like a photoemission process in which the plasmon plays the role of the photon with the exception that, depending on the plasmon momentum, nonvertical electronic transitions are possible [13].

When a monoenergetic electron beam of sufficiently high primary energy impinges on a metal surface, features associated with the excitation of plasmons are commonly observed in the kinetic-energy distribution of backscattered electrons. Plasmon energies in free-electron metals are of the order of 10–20 eV; thus, their decay often results in the emission of electrons in the low-kinetic-energy, or secondary-electron-energy, region of the spectrum. Unfortunately, the rather featureless spectrum associated with secondary electrons (SEs) prevents one from disentangling the contribution of the plasmon decay to the total secondary-electron spectrum. One possible way to overcome this drawback is to use an electron-electron coincidence spectroscopy. This technique consists of detecting correlated electron pairs. In the specific case discussed here, the sample is excited by means of an electron beam giving rise to a one-electron-in, two-electrons-out ($e,2e$) process. Backscattered electrons carry information about the excitation, in this case a plasmon, that was stimulated in the sample, while the emitted electrons provide information about the decay process.

Many experiments confirm the correlation between plasmon excitation and LEE emission [13–20]. In addition, ($e,2e$)

*gianluca.difilippo@uniroma3.it

spectroscopy has been proven to be very effective in disentangling secondary electrons generated by the decay of a selected plasmon excitation [13,19] and in highlighting the extreme surface sensitivity of the plasmon decay [20]. In those works it was pointed out that the energy and angle distribution of electrons emitted in coincidence with plasmon excitation is closely related to the band structure of the solid. It was additionally observed that the maximum of the plasmon decay cross section occurs when electrons from surface states are excited [19,20]. This is valid for both bulk and surface plasmons and suggests that the bulk plasmon oscillation also presents a nonvanishing intensity at the metal surface. That being the case, it raises the question of how the metal bulk plasmon decay is influenced by modification of the surface, such as the adsorption of an organic overlayer.

To this end we prepared a thin (4-Å) copper phthalocyanine (CuPc) layer on Al(111). We performed ($e,2e$) spectroscopy on both the clean and covered surfaces and observed the disappearance of the plasmon decay contribution to electron emission in the second case. This suggests that the influence of the bulk plasmon does not extend to the molecular layer but is confined in the half-space of the aluminum crystal.

II. EXPERIMENTAL DETAILS

The coincidence setup has been described in more detail elsewhere [13,20]. Thus, we recall here only the fundamental aspects of the experiment that are illustrated in Fig. 1. In the ($e,2e$) experiment the sample is excited by means of an electron beam of energy $E_0 = 103$ eV. The electron pairs are detected by means of two hemispherical analyzers. The first one (analyzer 1) is used to detect the backscattered electrons at kinetic energies within several eV of the primary beam energy, while the second one (analyzer 2) scans over the SE spectrum. The accepted polar angles are $\pm 1.0^\circ$ and $\pm 2.0^\circ$ for analyzers 1 and 2, respectively. The electron beam hits the sample with an angle $\theta_i = 15^\circ$ with respect to the normal to the surface. In order to maximize the coincidence intensity, a specular-reflection

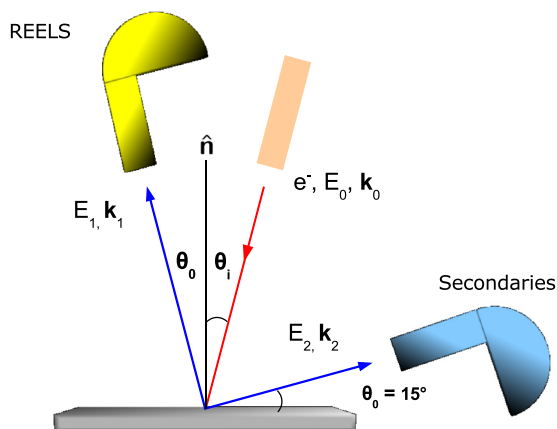


FIG. 1. Schematic of the experimental apparatus used to detect the reflected (analyzer 1) and secondary electrons (analyzer 2) in coincidence. A specular scattering geometry is adopted in which the reflected electrons have the same angle to the surface normal as the primary electrons ($\theta_o = \theta_i$).

geometry was employed where the incoming electrons are backscattered at an angle $\theta_o = \theta_i = 15^\circ$. The mutual angle between the analyzers is 90° , so that the takeoff angle of SE with respect to the sample surface equals θ_o . Analyzers 1 and 2 have an energy resolution of $\sigma_1 = 1.2$ eV and $\sigma_2 = 2.8$ eV, respectively. The total energy resolution for the coincidence experiment is given by $\sigma_{\text{coinc}} = \sqrt{\sigma_1^2 + \sigma_2^2}$ and amounts to 3.0 eV. The setup is additionally equipped with a He-discharge lamp ($h\nu = 21.2$ eV), a deuterium lamp ($h\nu = 4 - 10$ eV), and an Al K_α x-ray source ($h\nu = 1486.7$ eV) to perform valence-band and core-level photoemission experiments.

The Al(111) single crystal was cleaned by several cycles of Ar^+ -ion sputtering (1.5 keV) and annealing at 720 K. This procedure results in a very sharp low-energy electron diffraction pattern and x-ray photoemission spectroscopy (XPS) signal of common contaminants below the detection limit. The surface was oriented with the $\bar{\Gamma}-\bar{M}$ high-symmetry direction lying within the scattering plane defined by the wave vector of the incident (\mathbf{k}_0) and scattered (\mathbf{k}_1) electrons. CuPc films were grown *in situ* via sublimation of CuPc powder (prepared according to the method described in Ref. [21]) in a Knudsen-type evaporator held at a temperature of 570 K. The substrate was at room temperature during evaporation. In this condition the CuPc molecules are randomly oriented and do not form any ordered structure on the substrate. The evaporation rate was monitored by means of a quartz crystal microbalance and set to 0.25 Å/min. The thickness of the molecular layer was additionally checked via monitoring the intensity of the C 1s XPS line. The work function of the system decreases with the number of deposited molecules. It moves from 4.2 eV (clean aluminum) to 3.7 eV when the CuPc thickness grows up to 3 Å. This value does not change for larger CuPc thicknesses. This suggests that the completion of a CuPc monolayer (ML) is obtained at a thickness of 3 Å. Therefore, the coverage selected in this experiment (4 Å) corresponds to ~ 1.3 ML. The integrity of the CuPc film was constantly monitored, and no sign of degradation was observed during electron exposure. Despite that, the substrate cleaning procedure was repeated, and a new CuPc layer was evaporated every 48 h. The acquisition time of each point in the coincidence spectra is 5 h for the Al(111) and 16 h for CuPc/Al(111).

III. RESULTS AND DISCUSSION

A. Plasmon excitation

Figure 2 displays the electron-energy-loss (EEL) spectra of Al(111) (top) and 4-Å CuPc/Al(111) (bottom) obtained with a primary electron energy $E_0 = 103$ eV. The EEL intensity is reported as a function of the kinetic energy of the scattered electron (E_1 , bottom axis) and of the energy loss ($E_L = E_0 - E_1$, top axis). The experimental geometry is the same as that used in the coincidence experiment. The total energy resolution (source + analyzer) is 0.45 eV. The spectrum of Al(111) is dominated by two intense structures associated with the bulk ($E_L = 15.1 \pm 0.1$ eV) and surface ($E_L = 10.5 \pm 0.1$ eV) plasmons. A third peak at intermediate energy ($E_L = 13.0 \pm 0.2$ eV) corresponds to the excitation of a multipole surface plasmon (MP) [22], i.e., a surface

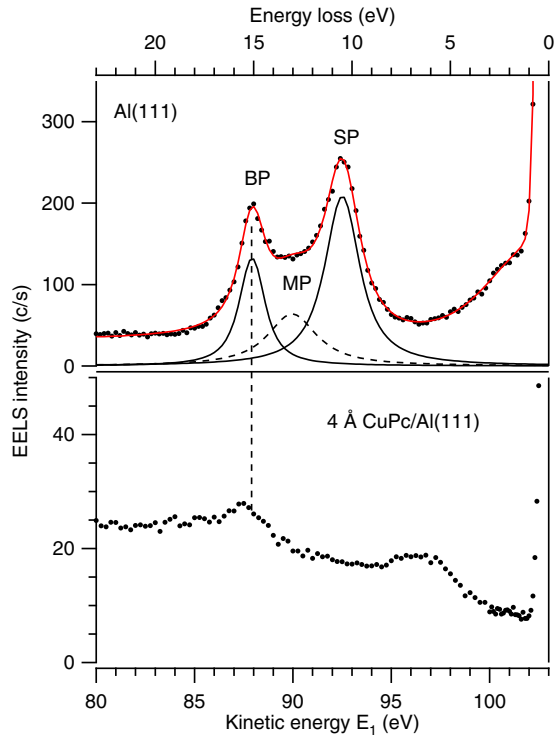


FIG. 2. Top: Electron-energy-loss spectrum of Al(111) (black points). The red solid line represents the best fit obtained by summing the contribution of surface (SP), bulk (BP), and multipole (MP) plasmons. Bottom: Electron-energy-loss spectrum of 4-Å CuPc/Al(111).

plasmon whose charge distribution has a multipole character [23]. A fourth structure appears on the low-energy loss side of the spectrum, and it corresponds to a quasivertical transition between occupied and unoccupied surface resonances close to the \bar{M} point of the Al(111) surface Brillouin zone [24].

The deposition of 4-Å CuPc leads to a sizable change in the EEL spectrum. The intensity of the BP is strongly attenuated, while the MP and SP loss features are not clearly discernible from the background. The evolution of the Al surface plasmon as a function of the CuPc thickness was already studied in a previous work [21]. At the early stages of the growth the SP energy shifts to lower values when the thickness of the molecular layer is increased. When the CuPc thickness grows up to 3 Å, the SP energy decreases to about 8 eV, and it is not possible to resolve it from the ($\pi \rightarrow \pi^*$) molecular transitions observed as a broad structure appearing between 4 and 8 eV energy loss. This behavior is ascribed to the formation of an interface plasmon, i.e., a surface plasmon wave propagating in the metal substrate whose energy is modified by the dielectric response of the CuPc layer [21].

The thickness of the molecular layer is such that contributions from the substrate (e.g., the bulk plasmon loss) are still detectable in the EEL spectrum. This is because the electron inelastic mean free path (IMFP) at the energies used in these measurements is large enough to let the backscattered electrons have a high probability of traveling through the molecular layer and reaching the vacuum without suffering an inelastic scattering. The IMFP of organic compounds can be calculated using the Tanuma, Powell, and Penn (TPP-2M)

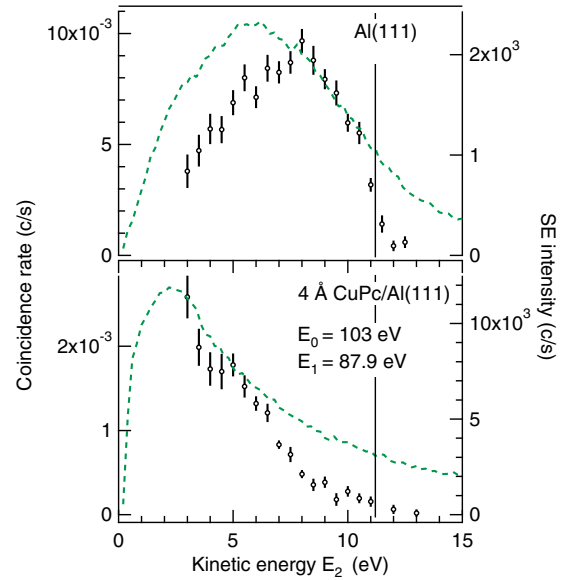


FIG. 3. Data points with error bars: SE spectrum measured in coincidence with the aluminum bulk plasmon loss feature of Al(111) (top) and 4-Å CuPc/Al(111) (bottom). The dashed green lines represent the corresponding SE spectra measured by analyzer 2 alone.

[25] formula. It turns out that for CuPc the IMFP of the backscattered electrons λ_{CuPc} corresponds to nearly 10 Å. This value is larger than the thickness of the molecular layer (4 Å) and ensures the possibility of obtaining information about the organic/inorganic interface. At the same time the small IMFP of Al ($\lambda_{\text{Al}} = 5.2$ Å) [26] ensures that more than 90% of the detected electrons are backscattered from a depth $\lesssim 10$ Å from the interface. Moreover, the high surface sensitivity of electron-energy-loss spectroscopy is additionally increased in the ($e, 2e$) experiment, as observed in all electron-electron coincidence experiments [17,27,28]. The bulk plasmons selected by the coincidence experiments discussed in the next section are therefore generated in the first atomic planes of the metal substrate. This results in the largest superposition between the bulk plasmon electric field and molecular electrons wave functions. This superposition is an essential condition to observe the emission of electrons from the CuPc layer driven by bulk plasmon decay [29].

B. Plasmon decay

Figure 3 shows the secondary-electron spectra (dashed line) of the clean Al(111) surface (top) and of 4-Å CuPc/Al(111) (bottom) produced when the surfaces are exposed to an electron beam with a primary energy of 103 eV. The CuPc spectrum is peaked at low kinetic energy ($E_2 \leq 3$ eV), and its intensity decreases at higher energy. The Al(111) spectrum presents a broader shape with a maximum around $E_2 = 6$ eV.

The fact that differences are observed between the spectra of the clean and covered surfaces is not surprising because the emission of SE is a material-dependent phenomenon. For example, it depends on the density of occupied and unoccupied electronic states of the system [30,31] and on the morphology of its surface [32]. In addition LEEs generated in plasmon decay processes also contribute to the SE spectrum. However,

noncoincidence measurements alone are not sufficient to determine the origin of the observed differences.

Figure 3 also shows coincidence spectra (circles with error bars) obtained when the analyzer detecting the backscattered electrons is set to the characteristic energy of the aluminum bulk plasmon ($E_1 = 87.9$ eV) while the second analyzer scans the SE spectrum ($3 \leq E_2 \leq 13$ eV). The coincidence rate is reported as a function of the kinetic energy of the emitted electrons. The spectrum of the clean aluminum surface (top panel) differs from the corresponding SE spectrum. The coincidence rate increases with the kinetic energy of the emitted electron and reaches its maximum value of 1×10^{-2} Hz at $E_2 = 8$ eV. For higher energies the intensity suddenly decreases, and it vanishes for $E_2 > 12$ eV.

Previous work has shown that a relevant plasmon decay channel proceeds through the formation of a single electron-hole pair [13,19,20]. In other words the $(e,2e)$ process can be interpreted in terms of a scattering event in which the energy and momentum of the excited plasmon are transferred to one electron-hole pair when the electron is emitted from the sample. Energy and momentum conservation laws have to be satisfied in this event:

$$E_2 = (E_0 - E_1) - E_b - \phi_A, \quad (1)$$

$$\mathbf{q}_{\parallel} = \mathbf{k}_{2\parallel} - \mathbf{k}_{p\parallel}. \quad (2)$$

Equation (1) asserts that the kinetic energy of the emitted electron E_2 corresponds to the difference between the energy lost by the scattered electron, $E_0 - E_1 = \hbar\omega_p$, and the binding energy in the initial state E_b . ϕ_A is the work function of the analyzer used to detect the low-energy electrons. Equation (2) ensures the conservation of the wave-vector component parallel to the surface. The wave vector of the target electron inside the sample \mathbf{q}_{\parallel} is given by the difference of the wave vector of the emitted electron $\mathbf{k}_{2\parallel}$ and that of the excited bulk plasmon $\mathbf{k}_{p\parallel}$. The latter corresponds to the momentum transferred by the incoming electron to excite the bulk plasmon.

Owing to the above-mentioned conservation laws, the coincidence spectrum can be correlated to the band structure of the investigated system. Figure 4 shows the electronic structure of Al(111) calculated by Heinrichsmeier *et al.* [24]. The light gray region is the projection of the bulk structure onto the surface. The dark gray region corresponds to a broad surface resonance. Sharper surface resonances are indicated by the solid circles connected by the black lines. Using Eqs. (1) and (2), we are able to determine the binding energy and crystal wave vector of the target electron for each point of the coincidence spectrum. These are represented by the orange squares superimposed on the electronic structure of Fig. 4. Each point is surrounded by a rectangular box accounting for energy resolution and wave-vector acceptance of the electron energy analyzers.

A comparison between the Al(111) band structure and the regions of the momentum-energy space explored by the coincidence experiment is useful to understand the cross section of the $(e,2e)$ process. In order to induce electron emission it is essential that occupied electronic states are available. Thus, we expect to have a high coincidence rate when the superposition between aluminum electronic states and portions of the momentum-energy space accessed by the experiment is

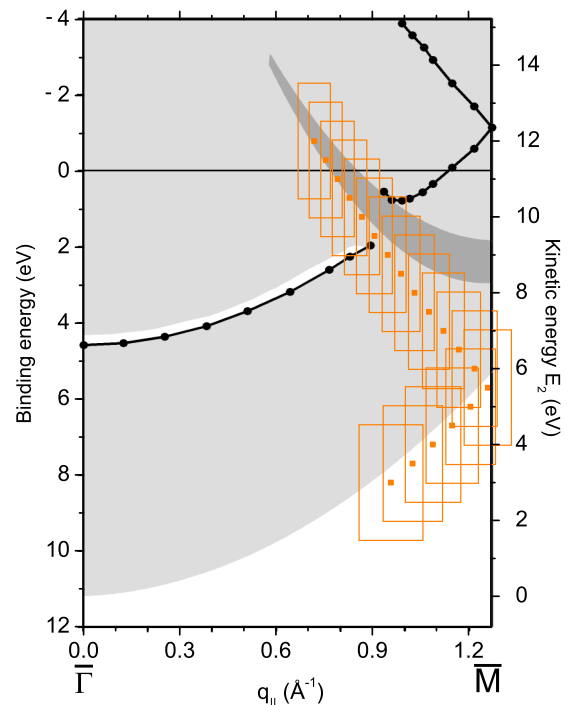


FIG. 4. Initial binding energy and momentum of LEE emitted in the decay of the Al(111) bulk plasmon (orange squares) obtained from Eqs. (1) and (2). The height and width of the rectangular boxes take into account energy and momentum resolution of the experimental setup. The kinetic energy of the emitted electron is indicated on the right axis. The background, adapted from Ref. [24], represents the calculated band structure of Al(111).

maximum. This is, indeed, the case for Al(111). The lowest coincidence intensity is observed at high ($E_2 > 11$ eV) and low ($E_2 < 4$ eV) kinetic energies of the emitted electron. The high-kinetic-energy onset observed in the spectrum at $E_2 = 11.2$ eV corresponds to the emission of electrons from the Fermi level, and it is indicated by the vertical line in Fig. 3. The intensity reduction at low kinetic energy corresponds to sampled regions falling in a projected band gap, where no electron is available for emission. The maximum of the $(e,2e)$ spectrum ($6 \leq E_2 \leq 10$ eV) is observed for initial binding energy and momentum of the emitted electron that fall in the projected bulk band of Al(111). In a previous work it was demonstrated that the aluminum bulk plasmon can decay through the emission of electrons from surface states [20]. This evidence suggests that the coincidence signal at $E_b < 3$ eV and $\mathbf{q}_{\parallel} > 0.7 \text{ \AA}^{-1}$ contains contributions from both bulk states and the broad surface resonance. This is because the electric field of the bulk plasmon has nonvanishing intensity at the surface. This suggests that in principle it might extend beyond the interface between the metal and the molecular layer in the CuPc/Al case.

The $(e,2e)$ spectrum of CuPc/Al(111) (bottom panel) differs drastically from the one of the clean substrate. The coincidence intensity is reduced by nearly five times, and it reaches its maximum value (2.5×10^{-3} Hz) at the lowest scanned kinetic energy ($E_2 = 3$ eV). The signal strongly decreases towards higher kinetic energies and vanishes above the Fermi energy threshold located at $E_2 = 11.2$ eV. In order to understand

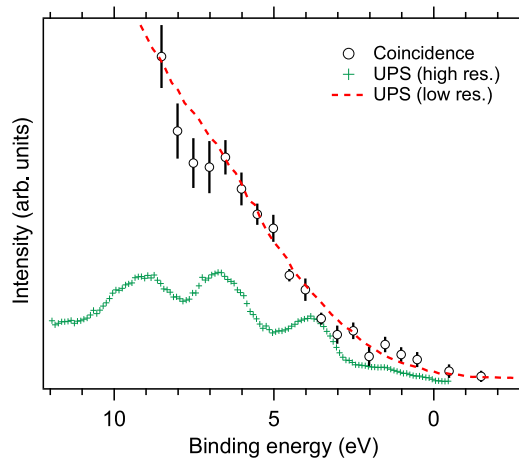


FIG. 5. SE spectrum of CuPc/Al(111) measured in coincidence with the Al bulk plasmon energy-loss feature and reported with dependence on the emitted electron binding energy obtained from Eq. (1) (open circles with error bars). The green crosses represent the corresponding valence-band photoemission spectrum. An analogous photoemission spectrum acquired at a resolution comparable with the coincidence experiment is represented by the dashed red line.

the origin of the coincidence spectrum of the molecular film it is helpful to compare it to the corresponding ultraviolet photoemission spectrum (UPS). Figure 5 shows the UPS spectrum of 4-Å CuPc/Al(111) measured using HeI radiation (green crosses). The origin of the different structures of the photoemission spectrum has been discussed elsewhere [33]. Here we just highlight the presence of several molecular levels. The CuPc highest occupied molecular orbital is observed as a weak structure at a binding energy of 1.5 eV. Lower-lying occupied molecular orbitals give rise to the three structures observed in the binding energy range from 3 to 10 eV. When the resolution of the analyzer is degraded to the value used in the coincidence measurement ($\sigma = 3$ eV), the photoemission spectrum results in the red dashed curve monotonically decreasing towards lower binding energies. For comparison the CuPc coincidence spectrum of Fig. 3 is plotted as a function of the emitted electron binding energy E_b obtained from (1) (open circles). It is evident that the coincidence and photoemission line show no remarkable difference. These results suggest that the measured ($e, 2e$) spectrum can be understood in terms of the emission of electrons from occupied molecular orbitals. The equivalence between the energy and momentum distribution of ($e, 2e$) and photoemission cross sections was already pointed out for metallic surfaces [34,35]. Due to its high surface sensitivity, ($e, 2e$) spectroscopy was used to determine the energy and momentum distribution of two surface states of W(001) [34] and of an oxygen-induced state of O/W(001) [35]. As a first result our experiment confirms that the coincidence technique can be additionally employed to study the electronic structure of thin films of organic molecules.

Once it is clear that the CuPc/Al(111) ($e, 2e$) spectrum is dominated by the emission of electrons from the molecular film, we want to determine the contribution of the plasmon excitation to the CuPc ionization. This is done via recording coincidence spectra in which the sum energy of the detected

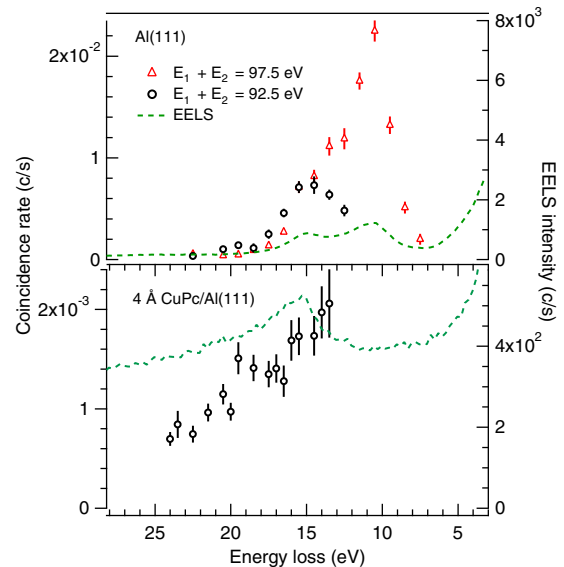


FIG. 6. Data points with error bars: electron-electron coincidence spectra of Al(111) (top) and 4-Å CuPc/Al(111) (bottom) obtained at $E_1 + E_2 = 97.5$ eV (open triangles) and $E_1 + E_2 = 92.5$ eV (open circles). The coincidence spectra are compared to the corresponding energy-loss spectra (dashed green line).

electrons, $E_{\text{sum}} = E_1 + E_2$, is kept constant. According to the energy conservation law of (1), the electron sum energy corresponds to the difference between the energy of the incoming electron ($E_0 = 103$ eV) and the binding energy of the target electron E_b . Thus, in constant-sum-energy spectra the binding energy of the emitted electron is fixed. In this condition two possible mechanisms can contribute to the coincidence intensity. When the energy lost by the backscattered electron is higher than plasmons' energies, LEEs can be emitted only by direct electron-electron scattering. In this case no plasmon is excited, and the scattered electron directly transfers part of its energy and momentum to a bound electron. For energy losses close to plasmons' excitation energies the contribution of plasmon decay adds a second channel in addition to the one of direct scattering. The results of the constant-sum-energy measurements are reported in Fig. 6, where the coincidence rate (symbols with error bars) is plotted as a function of the energy loss of the scattered electron. For comparison the corresponding EEL spectrum, recorded under the same conditions used in the coincidence experiment, is shown (dashed line). Two different sum energies were investigated, $E_{\text{sum}} = 92.5$ and 97.5 eV. Those were selected to detect electrons emitted from occupied states at $E_b = 6.3 \pm 1.5$ eV and $E_b = 1.3 \pm 1.5$ eV, respectively. In the former case (circles) the selected binding energy corresponds to occupied electronic levels in both the aluminum substrate and the CuPc overlayer. This is an ideal choice to compare the contributions of plasmon decay between the clean and covered surfaces. However, owing to energy conservation only electrons associated with the bulk plasmon excitation can be detected (the surface plasmon energy is not large enough to emit electrons from states at binding energy higher than 6 eV). In order to investigate the contribution of surface plasmon decay in Al(111) a lower binding energy ($E_b = 1.3$ eV) has also been considered (top panel, triangles).

It is evident that the $(e,2e)$ cross section of the clean surface resonantly increases when the energy loss of the incoming electron corresponds to the energy of surface and bulk plasmons. This effect was already observed by Samarin *et al.* [15] and by us [19] in earlier works on LiF and Be(0001), respectively. This means that the contribution of direct electron-electron scattering is negligible when compared to the contribution associated with plasmon decay. In addition the surface plasmon contribution to the $(e,2e)$ signal is higher than the bulk plasmon one. This difference cannot be related to the initial state of the scattering process. In fact, the regions of the momentum-energy space accessed at the characteristic energy loss of bulk and surface plasmons are located in an analogous portion of the projected Al band structure. In both cases electrons from bulk states and from the broad surface resonance are excited. Thus, the increased surface signal is most likely related to the extreme surface sensitivity of $(e,2e)$ spectroscopy. The electric field associated with the surface plasmon has maximum intensity at the surface; therefore, the detection of LEEs generated in the decay of surface plasmons is favored in the coincidence experiment.

The bottom panel of Fig. 6 shows the coincidence spectrum of CuPc/Al(111) obtained for $E_1 + E_2 = 92.5$ eV. The $(e,2e)$ spectrum does not show the same resonant behavior as Al(111). The coincidence signal monotonically increases towards lower energy loss, and it is not enhanced upon matching the bulk plasmon excitation energy. This implies that the $(e,2e)$ signal is essentially associated with direct electron-electron scattering, and plasmon decay via emission of LEEs from the molecular layer is not observed. Although bulk plasmons have been demonstrated to be able to decay through surface states of the system in which they have been excited, it is evident that they do not decay through states of the molecular overlayer, not even when the organic film thickness is smaller than the wavelength of the field associated with the bulk plasmon, $\lambda_p = 16$ Å. The current measurements cannot fully illuminate the reason behind this effect, but we will try to give a tentative explanation in the following. Nonradiative plasmon decay is a quantum-mechanical process in which the plasmon-induced electric field, which represents a time-dependent perturbation on valence electrons, can induce the generation of one electron-hole pair and, eventually, the emission of a low-energy electron [36]. In analogy to photoemission the transition matrix element depends on the scalar product of the plasmon vector potential and the electron-hole dipole moment [29]. Thus, the transition probability depends on the relative orientation of the two vectors and on their amplitude. In the performed experiment the first contribution is averaged and does not play a major role. This is because the CuPc molecules are randomly oriented onto the aluminum surface. In this condition, the fact that we do not observe any contribution related to plasmon decay in the coincidence spectrum of CuPc is most likely a consequence of the fact that the bulk plasmon vector potential (and hence electric field) intensity is strongly reduced in the molecular overlayer.

Pinchuk and Kreibig studied the damping of the surface plasmon in metallic nanoparticles [37]. They observed that the plasmon line is broadened when molecules are adsorbed on their surface. This effect is related to the presence of an additional plasmon decay channel due to molecule-induced

unoccupied states just above the metal Fermi level [37]. The presence of these states makes it possible for the plasmon electrons to penetrate into the molecular layer and then be reflected back into the metal. The penetration and reflection process adds additional phase shifts to the involved electrons and leads to a damping of the plasmon mode due to a pure dephasing process. The latter involves elastic scattering and leads to only a destruction of the phase coherence of the plasmon wave without any electron emission. The pure dephasing contribution to the plasmon lifetime depends on the position and width of the induced states and on the polarizability of the adsorbed molecules [37]. All of these parameters are related to the strength of the interaction between the substrate and the molecules. Earlier studies of CuPc films on aluminum showed a strong interaction at the interface which results in a charge transfer from the substrate to the organic film in the early stages of the growth [38]. This leads to the formation of a partially filled band resulting from the hybridization of the CuPc lowest unoccupied molecular orbital and aluminum states close to the Fermi level. The induced interface state might be responsible for the enhancement of the pure dephasing of the plasmon wave (at the interface) at the expense of the electron-hole pair generation channel. Note, however, that this is a tentative explanation and our experimental results do not determine the exact cause behind the lack of interaction between the metal bulk plasmon and the molecular electrons. In order to get a deeper understanding of the observed phenomenon theoretical calculations will be essential. Additional experiments performed on different overlayers (e.g., organic systems with different electronic structures and polarizabilities) will also be useful to determine the effect of the electronic properties of the molecules on the decay process.

IV. SUMMARY AND CONCLUSIONS

We studied the spatial localization of the aluminum bulk plasmon looking at the low-energy electron emission of a thin CuPc layer on Al(111). LEE emission and plasmon excitation are bound together by nonradiative plasmon decay, a process resulting in the emission of low-energy electrons. The measured $(e,2e)$ spectra of CuPc/Al(111) revealed that LEE emission is dominated by direct electron-electron scattering. In this regime the energy distribution of the $(e,2e)$ signal resembles the one observed in photoemission experiments, without any trace of cross-section enhancement at energy losses corresponding to the bulk plasmon frequency. This is clear evidence of the $(e,2e)$ cross section being dominated by direct dipolar scattering of the incoming electron with the molecules deposited onto the Al surface.

The absence of the contribution associated with plasmon decay in the SE spectrum of CuPc implies that the interaction of the aluminum bulk plasmon with the electrons in the molecular adsorbate does not lead to the emission of low-energy electrons. We speculate that this is due to the fact that the plasma oscillation is confined within the half-space of the Al crystal and its wave function vanishes or is strongly damped beyond the organic/inorganic interface. We tentatively

ascribe this result to the electronic properties of the molecular adsorbate that might lead to a shortening of the dephasing time of the electronic collective motion at the interface.

Additional experiments on different metal substrates and different organic molecules will be helpful to determine if this effect is a property of the investigated system or if this is a general property of metal/organic interfaces.

ACKNOWLEDGMENTS

Partial financial support through SIMDALEE2 Sources, Interaction with Matter, Detection and Analysis of Low Energy Electrons 2 Marie Skłodowska Curie FP7-PEOPLE-2013-ITN Grant No. 606988 is greatly acknowledged. R.A.B. acknowledges support from the NSF through Grant No. CHE1213727.

-
- [1] D. Pines, *Rev. Mod. Phys.* **28**, 184 (1956).
- [2] H. Raether, *Excitation of Plasmons and Interband Transitions by Electrons* (Springer, Berlin, 1980).
- [3] W. L. Barnes, A. Dereux, and T. W. Ebbesen, *Nature (London)* **424**, 824 (2003).
- [4] J. M. Luther and J. L. Blackburn, *Nat. Photonics* **7**, 675 (2013).
- [5] R. K. Vinnakota and D. A. Genov, *Sci. Rep.* **4**, 4899 (2014).
- [6] H. A. Atwater and A. Polman, *Nat. Mater.* **9**, 205 (2010).
- [7] T. Kume, S. Hayashi, and K. Yamamoto, *Jpn. J. Appl. Phys.* **32**, 3486 (1993).
- [8] T. Wakamatsu, K. Saito, Y. Sakakibara, and H. Yokoyama, *Jpn. J. Appl. Phys.* **36**, 155 (1997).
- [9] J. Homola, S. S. Yee, and G. Gauglitz, *Sens. Actuators B* **54**, 3 (1999).
- [10] S. Mukherjee, F. Libisch, N. Large, O. Neumann, L. V. Brown, J. Cheng, J. B. Lassiter, E. A. Carter, P. Nordlander, and N. J. Halas, *Nano Lett.* **13**, 240 (2013).
- [11] C. Clavero, *Nat. Photonics* **8**, 95 (2014).
- [12] S. Linic, P. Christopher, and D. B. Ingram, *Nat. Mater.* **10**, 911 (2011).
- [13] W. S. M. Werner, A. Ruocco, F. Offi, S. Iacobucci, W. Smekal, H. Winter, and G. Stefani, *Phys. Rev. B* **78**, 233403 (2008).
- [14] F. J. Pijper and P. Kruit, *Phys. Rev. B* **44**, 9192 (1991).
- [15] S. Samarin, J. Berakdar, A. Suvorova, O. Artamonov, D. Waterhouse, J. Kirschner, and J. Williams, *Surf. Sci.* **548**, 187 (2004).
- [16] W. S. M. Werner, F. Salvat-Pujol, W. Smekal, R. Khalid, F. Aumayr, H. Störi, A. Ruocco, and G. Stefani, *Appl. Phys. Lett.* **99**, 184102 (2011).
- [17] W. S. M. Werner, F. Salvat-Pujol, A. Bellissimo, R. Khalid, W. Smekal, M. Novák, A. Ruocco, and G. Stefani, *Phys. Rev. B* **88**, 201407 (2013).
- [18] M. Schüler, Y. Pavlyukh, P. Bolognesi, L. Avaldi, and J. Berakdar, *Sci. Rep.* **6**, 24396 (2016).
- [19] G. Di Filippo, D. Sbaraglia, A. Ruocco, and G. Stefani, *Phys. Rev. B* **94**, 155422 (2016).
- [20] A. Ruocco, W. S. M. Werner, M. I. Trioni, S. Iacobucci, and G. Stefani, *Phys. Rev. B* **95**, 155408 (2017).
- [21] A. Ruocco, M. P. Donzello, F. Evangelista, and G. Stefani, *Phys. Rev. B* **67**, 155408 (2003).
- [22] Any attempt to fit the EEL spectrum without the multipole plasmon component failed in reproducing the experimental data, especially in the region included between the two main loss features. In this region the theoretical curve consistently underestimates the experimental data. Including a third plasmon peak into the fitting function improves the reduced χ^2 value from 4.2 to 1.2.
- [23] G. Chiarello, V. Formoso, A. Santaniello, E. Colavita, and L. Papagno, *Phys. Rev. B* **62**, 12676 (2000).
- [24] M. Heinrichsmeier, A. Fleszar, and A. Eguiluz, *Surf. Sci.* **285**, 129 (1993).
- [25] S. Tanuma, C. J. Powell, and D. R. Penn, *Surf. Interface Anal.* **21**, 165 (1994).
- [26] J. Ashley, *J. Electron. Spectrosc. Relat. Phenom.* **50**, 323 (1990).
- [27] G. Stefani, R. Gotter, A. Ruocco, F. Offi, F. D. Pieve, S. Iacobucci, A. Morgante, A. Verdini, A. Liscio, H. Yao, and R. Bartynski, *J. Electron. Spectrosc. Relat. Phenom.* **141**, 149 (2004).
- [28] W. S. M. Werner, W. Smekal, H. Störi, H. Winter, G. Stefani, A. Ruocco, F. Offi, R. Gotter, A. Morgante, and F. Tommasini, *Phys. Rev. Lett.* **94**, 038302 (2005).
- [29] R. Sundararaman, P. Narang, A. S. Jermyn, W. A. Goddard III, and H. A. Atwater, *Nat. Commun.* **5**, 5788 (2014).
- [30] R. F. Willis, B. Fitton, and G. S. Painter, *Phys. Rev. B* **9**, 1926 (1974).
- [31] G. Chiarello, R. Agostino, A. Amoddeo, L. Caputi, and E. Colavita, *J. Electron. Spectrosc. Relat. Phenom.* **70**, 45 (1994).
- [32] B. L. Thiel and M. Toth, *J. Appl. Phys.* **97**, 051101 (2005).
- [33] F. Evangelista, V. Carravetta, G. Stefani, B. Jansik, M. Alagia, S. Stranges, and A. Ruocco, *J. Chem. Phys.* **126**, 124709 (2007).
- [34] S. Samarin, R. Herrmann, H. Schwabe, and O. Artamonov, *J. Electron Spectrosc. Relat. Phenom.* **96**, 61 (1998).
- [35] S. Samarin, J. Berakdar, R. Herrmann, H. Schwabe, O. Artamonov, and J. Kirschner, *J. Phys. IV* **09**, 137 (1999).
- [36] M. L. Brongersma, N. J. Halas, and P. Nordlander, *Nat. Nanotechnol.* **10**, 25 (2015).
- [37] A. Pinchuk and U. Kreibig, *New J. Phys.* **5**, 151 (2003).
- [38] A. Ruocco, F. Evangelista, R. Gotter, A. Attili, and G. Stefani, *J. Phys. Chem. C* **112**, 2016 (2008).